Molecular Orbital Model for Ion Polar-Molecule Capture Collisions

Ming Xu,[†] Stephanie Dillon,[†] J. Daniel Kimel,[‡] and Ralph C. Dougherty*,[†]

Departments of Chemistry and Physics, Florida State University, Tallahassee, Florida 32306-4390

Received: February 9, 2000; In Final Form: April 18, 2000

This article presents a molecular orbital model for ion polar molecule capture collisions which was developed by building on classical theoretical treatments. We replace the polarization potential with a perturbation molecular orbital potential, and assume that the molecular dipole does not change as a result of electron exchange at distances greater than or equal to the critical radius in the collision complex. Overlap integrals are introduced in this treatment of ion−molecule collision rates. For calculation of the perturbation molecular orbital potential, the overlap integral is approximated by use of Gaussian wave functions with scaled Slater atomic radii. The molecular dipole is assumed to be "locked" by the ion at the critical radius. The rotational mode of the molecular dipole along the locked axis is excited by coupling with the ion−molecule motion. The gain in rotational energy by the molecular dipole under the torque of the ion is approximated by a first-order Stark effect. Use of a Stark effect model results in the conservation of both energy and angular momentum. The net contribution of the ion−dipole interaction potential to ion−molecule capture collisions is to remove the rotational energy of the ion and dipole. The decrease in the ion polar molecule interaction potential caused by Stark effect excitation of dipole rotation accounts for the fact that the locked dipole approximation without Stark effect coupling significantly overestimates the rates of ion polar molecule collisions. Ab initio molecular orbital calculations on model systems were conducted to convert Slater atomic orbital radii into approximate molecular orbital radii by evaluating a scaling parameter, *f*. Experimental hydride transfer rates reflect the convolution of collision rates and subsequent hydride transfer rates. The reaction efficiency for hydride transfer is the ratio of the experimental reaction rate divided by the collision rate. Reaction efficiencies obtained using the collision model developed here are in qualitative agreement with Golden Rule reaction rate models. This result is in contrast with reaction efficiencies calculated by classical potentials that show a monotonic increase in reaction efficiency with increasing reaction free energy.

Introduction

Early in this century Langevin introduced a model for ion−molecule collisions based on a point charge and a point-polarizable molecule.[1] This theory was subsequently elaborated and reformulated by several authors.[2,3] The presence of a permanent dipole moment introduces strongly anisotropic ion−dipole interactions and significantly complicates the calculation of an attraction potential. A variety of theoretical treatments have been introduced to address ion−dipole interactions. Averaged dipole orientation (ADO) theory[4] may be the best known and most widely used of these theories. Advances on this theory have included many new models. The names of these models are descriptive of their focus: angular momentum corrected ADO theory,[5] spherically averaged energy model,[6] free energy treatment model,[7] trajectory calculation model,[8] adiabatic invariance method,[9] semiclassical perturbed rotational state model,[10] and statistical adiabatic channel model.[11] All these models predict collision rates using a polarization potential modified by a cos θ dependence for the ion−dipole interaction term. In the spherically averaged energy model,[12] Baker and Ridge introduced the Langevin function in the treatment of the ion−dipole interaction term.

The Stark effect is the splitting of the lines in the microwave spectrum when gaseous polar molecules are examined in an electric field.[13] The effect is due to the interaction of the dipole moment of a gas molecule and an electric field. Following the formalism developed by Baker and Ridge,[6] we will begin with the Stark effect in our examination of ion and dipole interactions.

We first develop the treatment of the interaction potential between an ion and a nonpolar molecule, which is a part of all ion molecule capture collisions. The ion nonpolar molecule potential is assumed to be independent of the ion−dipole interaction terms both in classical treatments and in the treatment presented here.

Molecular Orbital Model for Ion Nonpolar Molecule Capture Collisions

When the attraction potential between an ion and molecule is sufficient to cause ion−molecule capture and subsequent reaction, the attraction potential is a first-order molecular orbital effect.[14] The attraction potential, ΔE_{DA}, between the ion and the molecule is given by eq 1.[13]

$$\Delta E_{DA} = n_o d_{oD} a_{oA} \beta_{DA} \tag{1}$$

where n_o is the number of electrons in the highest occupied orbital of the ion−molecule complex, d_{oD} and a_{oA} are the frontier orbital coefficients at the reaction site for the donor and acceptor, and β_{DA} is the resonance integral for bond formation between the donor and acceptor. In a cation−molecule complex the bond-forming interaction is between the vacant orbital of the cation and the highest occupied orbital of the neutral. In an anion−

* To whom correspondence should be addressed: ralphd@chem.fsu.edu.
[†] Department of Chemistry.
[‡] Department of Physics.

10.1021/jp0005266 CCC: $19.00
Published on Web 07/21/2000

molecule complex the bond-forming interaction is between the lowest vacant orbital of the molecule and the highest occupied orbital of the anion.

The Mulliken approximation for the resonance integral uses the average of the orbital energies for the frontier orbitals of the reactive species (eq 2).[15]

$$\beta_{DA} = cS_{DA}(\text{average frontier orbital energy}) \qquad (2)$$

Here c is a constant (set to 1.0) and S_{DA} is the overlap integral for the donor and acceptor frontier orbitals. For an anion−molecule complex the appropriate orbitals are the highest occupied orbital of the anion and the lowest vacant orbital of the neutral. The energies of these orbitals can be approximated by the negative of the electron affinity corresponding to production of the anion and the negative of the electron affinity of the neutral. For cation−molecule complexes the appropriate orbitals are the highest occupied orbital of the neutral and the lowest vacant orbital of the cation. These orbital energies can be approximated by the negative of the ionization potential of the neutral member of the complex and the negative of the ionization energy of the neutral corresponding to the cation.

Replacing the classical polarization potential with the perturbation molecule orbital (PMO) ion molecule potential for ion nonpolar molecule collisions, ΔE_{DA}, the central effective potential becomes:

$$V_{eff} = \frac{L^2}{2\mu r^2} - \Delta E_{DA} \qquad (3)$$

Once the appropriate orbital energies have been determined, it is only necessary to obtain the overlap integrals to evaluate the effective potential, V_{eff}. Gaussian spherical orbitals have the form:

$$\Psi_i = N_i \exp\left(\frac{-r^2}{a_i^2}\right) \qquad (4)$$

Here N_i is the normalization constant, r is the electron coordinate relative to the atomic center at the origin, and a_i is the orbital radius. We use spherical orbitals to represent both the ion and the molecule. This was done primarily for simplicity in calculation. For small molecules this approximation is not extreme. For larger molecules with complex shapes or for complex polyatomic ions, it will be necessary to use a different approximation. Using the Gaussian wave functions, eq 4, we obtain the overlap integral (eq 5).

$$S_{DA} = \left[\frac{2a_i a_m}{a_i^2 + a_m^2}\right]^{3/2} \exp\left[\frac{-r^2}{a_i^2 + a_m^2}\right] \qquad (5)$$

Orbital energies are correlated with orbital radii for spherical orbitals. Slater-type atomic orbital radii are directly related to orbital energy (eq 6).[16]

$$a_{MO} = fa_o n\left(\frac{E_H}{E}\right)^{1/2} \qquad (6)$$

a_{MO} is the molecular orbital radius; f is a molecular orbital scaling parameter, obtained here by ab initio calculations; a_o is the Bohr radius; E_H is the energy of a hydrogen 1s atomic orbital; E is the energy of the frontier orbital associated with the ion or molecule; N is the principal quantum number for the "spherical" molecular orbital. The molecular orbital scaling parameter, f, is needed to adjust the scaling in this approximate molecular orbital model. We obtain the value of this parameter by use of ab initio calculations of the ion molecule potential. The value of f is then adjusted to bring the PMO calculation into agreement with the ab initio calculation. The value of f for data in this manuscript has been set to 1.6 using comparisons of PMO and ab initio collision rates.

Using eq 6 for the molecular orbital radius, the ion−molecule overlap integral, S_{IM}, and potential, V_{IM}, become:

$$S_{IM} = \left[\frac{2n_I n_M (E_I E_M)^{1/2}}{(n_I^2 E_M + n_M^2 E_I)}\right]^{3/2} \exp\left[\frac{-r^2}{f^2 a_o^2 E_H\left(\frac{n_I^2}{E_I} + \frac{n_M^2}{E_M}\right)}\right] \qquad (7)$$

$$V_{IM} = \Delta E_{IM} = A \exp\left(\frac{-r_c^2}{B^2}\right) \qquad (8)$$

$$A = \left[\frac{2n_I n_M (E_I E_M)^{1/2}}{(n_I^2 E_M + n_M^2 E_I)}\right]^{3/2} (E_I + E_M)$$

$$B = \left[f^2 a_o^2 E_H\left(\frac{n_I^2}{E_I} + \frac{n_M^2}{E_M}\right)\right]^{1/2}$$

The approximate molecular orbital potential (eq 8) uses the frontier orbital energies for the ion and molecule, E_I and E_M; the principal quantum numbers, n_I and n_M, associated with the orbitals on the ion and the molecule; the ion−molecule separation, r; and the orbital radius scaling parameter, f. This approximation to the ion−molecule Hamiltonian is an algebraic function. Once the calculation has been set up in a spreadsheet, or other calculating engine, the calculations are simple to perform.

The ion−molecule attraction potential has the greatest susceptibility to alteration caused by electron exchange. Dipole moments are much less susceptible to perturbation by electron exchange than polarizabilities. We have treated the ion−molecule potential with an approximate quantum mechanical function and all other potentials have been treated classically. In this treatment the ion−molecule orbital, translational, and rotational motions are treated classically.

We use Langevin capture criterion[17] with eq 3 to obtain the relative energy (eq 9), E_{rel}, in terms of the critical radius, r_c, the impact parameter (eq 10), b_c, and the collision rate constant (eq 11), k_{col}.

$$E_{rel} = \left(\frac{r_c^2}{B^2} - 1\right) A \exp\left(-\frac{r_c^2}{B^2}\right) \qquad (9)$$

$$b_c = \frac{r_c}{\sqrt{E_{rel}}}\sqrt{\left(\frac{r_c^2}{B^2}\right) A \exp\left(-\frac{r_c^2}{B^2}\right)} = \frac{r_c}{\sqrt{E_{rel}}}\sqrt{A \exp\left(-\frac{r_c^2}{B^2}\right) + k_B T} \qquad (10)$$

$$k_{coll} = u\sigma_c = \pi u b_c^2 = \pi r_c^2 \sqrt{\frac{2}{\mu E_{rel}}}\left(\frac{r_c^2}{B^2}\right) A \exp\left(-\frac{r_c^2}{B^2}\right) \qquad (11)$$

B is the term defined in eq 8. The relative translational velocity, u, is calculated from the reduced mass, μ, and the relative energy. The relative energy, E_{rel}, is assumed to be equal

to k_BT ($u = (2k_BT/\mu)^{1/2}$). We obtain the values of the critical radius, r_c, by a graphical method.

Negative and Positive Ions in the Model

Negative ion formation rates span a significantly larger range than the rates of corresponding positive ion reactive formation processes. It is possible to detect as few as 200 000 molecules (100 ag) of octafluoronaphthalene[18] in negative chemical ionization mass spectrometry. In a similar experiment, benzene is not detected when introduced at concentrations nearly a trillion times higher. These two molecules have roughly comparable sensitivities for reaction in positive chemical ionization ion formation processes with protonated methane as the reactive ion. The difference between the positive and negative ion−molecule collision rates depend more on orbital energies than on polarizabilities. If polarizability controlled the ion−molecule collision rates, the rates for proton and hydride collisions, or other isobaric pairs, with a given molecule would be the same. This would imply that benzene should be as easily detected in negative ion collisions as octaiodonaphthalene. In reality the negative ion sensitivities for benzene and octaiodonaphthalene differ by at least a factor of 10^{12}. Instead of polarizability, the frontier orbital energy controls the rates of ion−molecule collisions. Benzene has a negative electron affinity, whereas octaiodonaphthalene's electron affinity is positive.

The frontier reactive orbital on the molecule, for positive ion collisions, is the highest occupied molecular orbital (HOMO). The corresponding frontier orbital for negative ion collisions is the lowest unoccupied molecular orbital (LUMO). In a simplistic view, the switch of the collision-controlling orbital from the HOMO to the LUMO accounts for the differences in sensitivity of benzene and octafluoronaphthalene in positive and negative ion-forming processes.

Ionization energies, the energies of the HOMOs, for closed shell organic molecules generally range between 7 and 12 eV.[19] This relatively small range for frontier orbital energies accounts for the relatively small range in the rate of positive ion−molecule collision processes. In contrast, the electron affinities of closed shell organic molecules range from positive to negative values.[18] For molecules with negative electron affinities ion−molecule interactions are repulsive and the corresponding collision processes are slow and often difficult to observe.

The rates of negative ion−molecule reactions involving molecules with positive electron affinities and thermal electrons are increased substantially by the low mass of the electron as compared with the positive ion counterpart. The de Broglie wavelength of a thermal electron at 300 K is 7.63 nm. This is 10 times the radius of the LUMO of a small molecule ion. For resonance electron capture, only the electron affinity of the molecule and the overlap integral for the LUMO of the molecule and the free-electron wave function are involved in the effective ion molecule potential, V_{eff}. This means that the overlap integral contribution to the rate process will favor negative ion reactions by a factor of roughly 1000 compared with a positive ion counterpart. Negative ion processes are also favored because the energy of the LUMO on the reactive molecule and the free electron are generally much closer to each other than the corresponding energies for positive ion collision processes. First-order molecular orbital perturbations are maximized when the interacting orbitals are degenerant.[14]

Molecular Orbital Model for Ion Polar Molecule Collisions

In ion polar molecule collisions, one of the roles of the ion−dipole interaction is to increase the local concentration of reactants. Ion−dipole potentials, like the polarization potential, extend to very long distances (>100 Å) and bring ions and molecules together.

We used the following assumptions in developing the ion polar molecule collision model: (1) a polar molecule is regarded as a rigid dipole at ion−molecule distances greater than or equal to the critical radius, r_c; (2) the PMO potential between the ion and molecule is the only quantum potential, all other interactions (e.g., the ion−dipole potential) are treated classically; (3) at the critical radius the dipole orientation is 'locked' by the ion−dipole interaction; (4) for nonlinear molecules the dipole's rotation around the locked axis is excited by the ion−molecule interaction; and (5) the change in rotational energy is approximated by a first-order Stark perturbation. The first assumption is common to most other treatments of ion polar molecule collisions. The usual assumption for the potential (assumption 2) is that it is either a quantum potential or a classical potential. The assumption that the ion−dipole potential is classical does not differ from the assumption of a completely quantum potential, except at distances that are generally shorter than r_c. The basis for the assumption that the ion locks the orientation of the dipole (assumption 3) comes from ab initio calculations of ion−molecule geometries as a function of distance. All these calculations show that the locked geometry is the lowest in energy, as one would expect. Addition of thermal agitation will make this minimum fuzzy. It will not change its location.

In the absence of a mechanism for dissipation of the change in potential associated with the locked dipole (our assumption 5), the presence of a locked dipole would make the ion−molecule collision cross-section unrealistically large. We assume that the reduction of the impact of the dipole moment on the cross-section is caused by the operation of the Stark effect (assumption 5).

In the ADO treatment[4b,5,8e] the assumption that there is an average dipole orientation different from the locked geometry reduces the influence of the molecular dipole on the ion−molecule collision cross-section. This assumption cannot be correct. There is no mechanism for changing the orientation of the molecular dipole toward a gas-phase ion from an average angle of 0° (locked orientation) to a larger angle. On the other hand, the Stark effect is known to operate for gas-phase molecules.

We use the semiclassical Hamiltonian equation for ion−molecule collisions and replace the polarization potential with the molecular orbital potential (eq 12). In this case the corresponding central effective potential, V_{eff}, becomes (eq13):

$$H_r = \frac{p_r^2}{2\mu} + \frac{L^2}{2\mu r^2} + \frac{J^2}{2I} - A\exp\left(-\frac{r^2}{B^2}\right) - \frac{\mu_D q}{r^2} \qquad (12)$$

$$V_{eff} = \frac{L^2}{2\mu r^2} + \frac{\Delta J^2}{2I} - A\exp\left(-\frac{r^2}{B^2}\right) - \frac{\mu_D q}{r^2} \qquad (13)$$

Here H_r is the Hamiltonian for the radial motion, p_r is the radial momentum of the collision complex, μ is the reduced mass, L is the orbital angular momentum of the collision complex, J is the angular momentum of the dipolar rotor, I is its moment of inertia, r is the distance between the collision partners, μ_D is the molecular dipole moment, and q is the ion charge. Equation 13 for the central effective potential, V_{eff}, contains all the terms that explicitly depend on r. $\Delta J^2/2I$ represents the increment in dipole rotational energy from infinite separation to r.

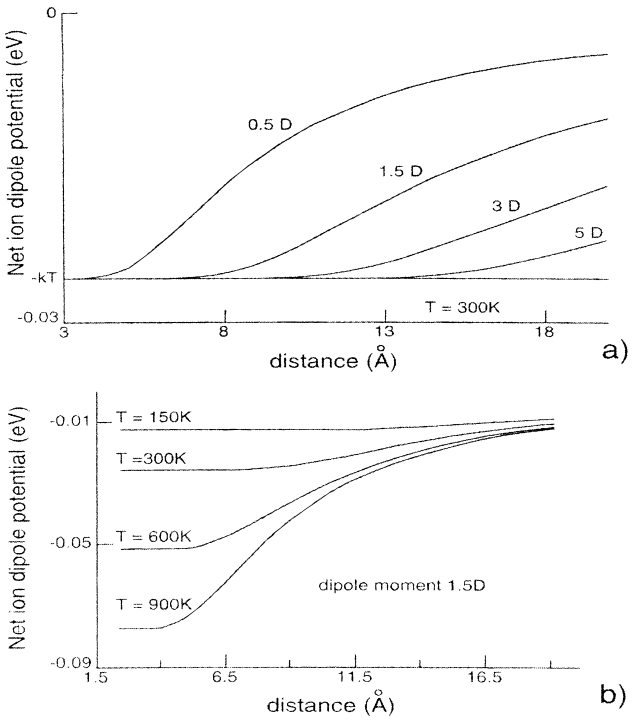

Figure 1. Net ion−dipole potential for (a) different dipole moments and (b) different temperatures as a function of ion−molecule distance.

We use the first-order Stark effect to approximate the gain in dipole rotational energy in ion polar molecule collisions. The ensemble averaged energy,[20] $\langle\phi\rangle$ is given by eq 14. In eq 14 L{x} is the well-known Langevin function. With linear polar molecules the rotational energy levels of the dipolar rotor lack the degeneracy necessary to produce a Stark effect.[12] For these molecules we assume that rotation of the dipole is not excited by the ion's electric field. The net contribution of the ion−dipole interaction potential to ion−molecule capture collisions is to remove the rotational energy gained

$$\langle\phi\rangle = -\left(\frac{\mu_D q}{r^2}\right) \mathrm{L}\left\{\frac{\mu_D q}{r^2 k_B T}\right\} \tag{14}$$

$$\mathrm{L}\{x\} = \frac{e^x + e^{-x}}{e^x - e^{-x}} - \frac{1}{x}$$

by the dipole rotor from the interaction potential energy of the ion and dipole. The decrease in the ion polar molecule interaction potential caused by the Stark effect excitation of dipole rotation accounts for the fact that the locked dipole approximation without Stark effect coupling significantly overestimates the rates of ion polar molecule collisions.[4,8] The dipole orientation in an ion polar molecule collision complex must be approximately locked at 0°, because the field strength needed to rotate a dipole is smaller than the field strength needed to cause an equivalent translation of the molecule. In ion polar molecule collisions the field strength due to the ion is sufficient to induce translation in molecules near the ion. The same field will definitely cause rotation of the molecular dipole to maximize the attraction potential between the ion and molecule.

The magnitude of the Stark effect perturbation on the ion−dipole potential as a function of dipole moment and temperature is illustrated in Figure 1a and 1b, respectively. The net ion−dipole potential, Figure 1, is given by eq 15.

$$V_{\text{ion-dipole-net}} = -\left(1 - \mathrm{L}\left\{\frac{\mu_D q}{r^2 k_B T}\right\}\right)\frac{\mu_D q}{r^2} \tag{15}$$

It would be possible to model these nonlinear functions with nonlinear parametric equations, but that modeling might disguise the basis for the conversion of orbital angular momentum to angular momentum of the dipole in the ion polar molecule complex.

A macroscopic mechanical analogue for the Stark effect coupling of the approximately orthogonal rotational motions in an ion−molecule collision complex is available in the form of a truncated spherical top attributed to Niels Bohr. These tops are available in several models from suppliers of scientific demonstration equipment. When spun with the spherical surface down the top will flip over and spin on its spindle. The flipping motion is accomplished at the expense of the rotational and precessional angular momentum of the top, both of which are approximately orthogonal to the flip axis.

Using the Stark effect to model the change in dipole rotor angular momentum, the net effective central potential is:

$$V_{\text{eff}} = \frac{L^2}{2\mu r^2} - A\exp\left(-\frac{r^2}{B^2}\right) - \left(1 - \mathrm{L}\left\{\frac{\mu_D q}{r^2 k_B T}\right\}\right)\frac{\mu_D q}{r^2} \tag{16}$$

By applying the Langevin capture criteria to this equation we can obtain the relative energy (eq 17), the impact parameter (eq 18), and the collision rate constant (eq 19). The critical radius, r_c, can be obtained graphically using the net effective central potential (eq 16) and the following expressions.

$$2E_{\text{rel}} = \left(\frac{r_c^2}{B^2} - 1\right) A\exp\left(-\frac{r_c^2}{B^2}\right) + \frac{\mu_D^2 q^2}{r_c^4 k_B T}\sinh^{-2}\left(\frac{\mu_D^2 q}{r_c^2 k_B T}\right) \tag{17}$$

$$b_c = \frac{1}{\sqrt{E_{\text{rel}}}}\sqrt{r_c^2\left(A\exp\left(-\frac{r_c^2}{B^2}\right) + k_B T\right) + \left(1 - \mathrm{L}\left\{\frac{\mu_D q}{r_c^2 k_B T}\right\}\right)\mu_D q} \tag{18}$$

$$k_{\text{col}} = u\sigma_c = \pi u b_c^{\,2} = k_{\text{PMO}} + k_{\text{ion-dipiole}} \tag{19}$$

We graphically solve eq 16 for the impact parameter, b_c, by

$$k_{\text{coll}} = \pi r_c^2\sqrt{\frac{2}{\mu E_{\text{rel}}}}\left(A\exp\left(-\frac{r_c^2}{B^2}\right) + k_B T\right) + \pi\sqrt{\frac{2}{\mu E_{\text{rel}}}}\left[\left(1 - \mathrm{L}\left\{\frac{\mu_D q}{r_c^2 k_B T}\right\}\right)\mu_D q\right]$$

setting the maximum value for the net effective central potential, V_{eff}, equal to $k_B T$. With the value of the impact parameter and the critical radius, it is possible to obtain the collision rate constant. The graphical solution of eq 16 for b_c is illustrated in Figure 2 for hydride transfer to ammonia. The electron affinity of ammonia is negative, which leads to a repulsive surface for the hydride ammonia encounter. For this graphic we have used the "virtual electron affinity" of ammonia, the electron affinity of NH_2, 0.75 eV. Access to this virtual state of ammonia requires electron tunneling. In solving eq 16 the orbital angular momentum, L, of the complex is approximated by μub, where μ is the reduced mass, u is the relative velocity, and b is the impact parameter. The expression comes from the classical Hamiltonian. With the assumption that the relative energy is

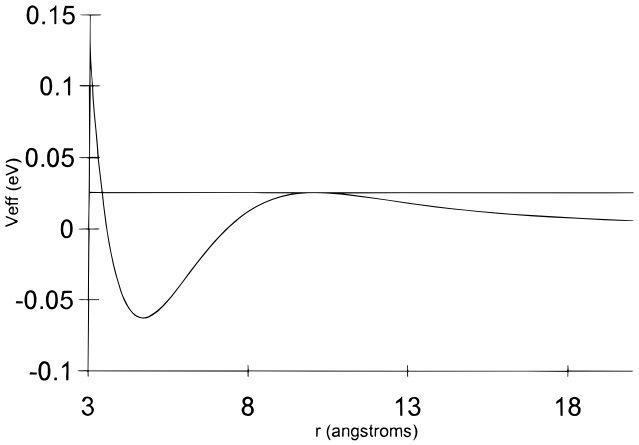

Figure 2. Graphical solution for r_c and b_c using eq 16 for hydride collision with ammonia (see text).

TABLE 1: Thermodynamic Data for Hydride Ion Proton Transfer Reactions $H^- + YH \rightarrow H_2 + Y^-$

target molecule YH	μ_D[21] (D)	products ions Y^-	EA[18] of Y^- (eV)	ΔG_{acid}[19] (kJ/mol)
HCN	2.98	CN^-	3.74	1438
CH_3NO_2	3.46	$CH_2NO_2^-$	0.49	1465
CH_3CN	3.92	CH_2CN^-	1.46	1528
C_2H_2	0.00	C_2H^-	3.73	1577
H_2O	1.85	HO^-	1.83	1607
$(CH_3)_2NH$	1.03	$(CH_3)_2N^-$	0.39	1628
$C_2H_5NH_2$	1.22	$C_2H_6NH^-$	0.66	1639
NH_3	1.47	NH_2^-	0.75	1657
		precursor ion		
		H^-	0.80	1649

equal to k_BT, the relative velocity is given by $(2k_BT/\mu)^{1/2}$. After setting up eq 16 in a spreadsheet as a graphic, we varied the value of b until the curve generated just touched k_BT (Figure 2).

Application of PMO Collision Theory to Ion Polar Molecule Collisions

A substantial body of data exists on hydride transfer reactions in anion−molecule collisions at relatively high pressures.[21] Reactions of anions are attractive for this initial work, because the free energy of reaction is sufficiently small that electronically excited states of product ions, or neutrals, are much less likely than in reactions of He^+ for example. The systems we have examined are listed in Table 1.

For reactions with $\Delta G°$ smaller than 1 eV in Tables 1 and 2, the electron affinity of the molecule is negative, and the molecule-hydride potential surface is uniformly repulsive. Thermal ion−molecule collisions, and hydride transfer reactions, in these cases, happen through tunneling to the reactive (attractive) state. To apply the model above to ion polar molecule capture collisions it is necessary to set the value of the orbital radius scaling parameter, f, that is used to determine the overlap integral. This parameter can be evaluated using ab initio calculations. The ab initio potential, $V_{ab\ initio}$ (eq 20), includes the ion−dipole contribution.

$$V_{eff} = \frac{L^2}{2\mu r^2} + L\left\{\frac{\mu_D q}{r^2 k_B T}\right\}\frac{\mu_D q}{r^2} - V_{ab\ initio} \qquad (20)$$

The ab initio potential was obtained using Gaussian 94[22] with an MP2/6-31+G(d) basis set. The potential was obtained by subtracting the optimized energy at a give distance between the mass centers of the collision pair from the energy at infinite separation (300 nm). The nuclear coordinates from the optimization placed the molecular dipole on the axis connecting the centers of mass (locked geometry). The geometry of the target molecule began to change significantly at 0.6 nm for H^-/H_2O, and at 0.9 nm for the other target molecules in Table 1. The impact parameter and critical radius were obtained for the ab initio values in Table 2 by adjusting the impact parameter so that V_{eff} (eq 20) was equivalent to k_BT. The results of these calculations are given in Table 2. The reaction efficiency, k_{exp}/k_{col}, is the gas-phase equivalent of the reaction rate in solution. This is because the collision rate in solution is independent of structure, and in the gas-phase collision rates strongly depend on structure. Modern theories of chemical reaction rates[23] give the log of the solution reaction rate as an approximate quadratic function of the reaction free energy. For the data and molecular orbital collision rate calculations in Table 2 this function is illustrated in Figure 3.

For the calculations reported in Tables 2 and 3, the orbital radius scaling parameter, f, was set to a value of 1.601. This value was obtained from the ab initio collision rate constant for the reaction between hydride and acetonitrile. The orbital radius scaling parameter was obtained by setting the rate constant for the PMO model equal to that obtained using the ab initio potential. This parameter was used for the entire series of reactions.

The overlap integral at the critical radius was nearly a factor of 10 higher for the polar molecules in Table 2 as compared with acetylene. The overlap integral for HCN was essentially the same as that for acetylene. HCN is a linear molecule. As a result it is not possible for the hydride electric field to excite rotation of the HCN.

In nonpolar molecules the ion−dipole potential term and the translational centrifugal term cancel at the critical radius using Langevin capture criteria. The critical radius is thus determined solely by the molecular orbital potential. When a molecule has a permanent dipole moment, the ion−dipole interaction contributes to the collision pair potential. The increase in the overall attraction causes a decrease in the critical radius and an increase in the overlap integral in the molecular orbital potential term.

We see no direct way to verify the collision rate because the experimental observation is the product of the collision rate times the reaction efficiency. Using the model described here it is possible to obtain reaction efficiencies that are fully in accord with Golden Rule kinetic theories.[23] Classical collision models often give reaction efficiencies greater than one.[13] Classically calculated collision rates also increase monotonically with reaction free energy (see Tables 2 and 3). It is well-known that increasing reaction free energy will cause an initial increase in reaction rate (efficiency) followed by a decrease.[23] The increase and decrease in rate (efficiency) is caused by the impact of the structural reorganization in the rate process. In this light, a series of reactions that show unit reaction efficiency for widely varying reaction free energies is neither physical nor reasonable. Reactions that have efficiencies greater than one are, of course, absurd.

The results in Tables 2 and 3 include calculations of ion−molecule collision rates using a classical model.[4b,8e] For these calculations the maximum value for k_{exp}/k_{coll} was obtained for HCN (1.4), the most exothermic reaction partner in the series.

In general the results for the classical calculations in Tables 2 and 3 paralleled the classical calculations reported by Bohme,[20] which showed an almost quantal shift in reaction efficiency

TABLE 2: PMO and ADO Capture Collision Rate Constants and Critical Radii for the Reactions $H^- + HY \rightarrow H_2 + Y^-$ at 297 K[a]

		r_c (nm)				k_{coll}			
reactant	k_{exp}[20]	PMO	G94	ADO[8e]	$S \times 10^2$	PMO	G94	ADO[8e]	$\Delta G°$ (eV)
HCN	15	0.90	0.92	0.52	0.2400	31.8	34.9	10.9	2.19
CH_3NO_2	13	1.02	0.97	0.61	3.339	21.3	28.6	13.0	1.91
CH_3CN	13	0.89	0.98	0.59	1.443	14.6	14.4	14.1	1.26
C_2H_2	4.4	0.92	0.94	0.56	0.2409	7.12	8.3	4.46	0.747
H_2O	3.7	0.87	0.61	0.44	1.027	13.8	10.9	7.11	0.436
$(CH_3)_2NH$	4.3	11.9		0.64	1.857	20.7		7.00	0.218
$C_2H_5NH_2$	1.1	1.04		0.64	1.568	17.5		7.32	0.104
NH_3	9.2×10^{-4}	0.99		0.5	1.358	17.5		6.46	−0.083

[a] k_{exp}, the experimental reaction rate constant (10^9 $mol^{-1}\cdot cm^3\cdot s^{-1}$). [b] k_{MO}, k_{PMO}, the calculated (PMO or Gaussian-94) collision rate constants (10^9 $molecule^{-1}\cdot cm^3\cdot s^{-1}$).

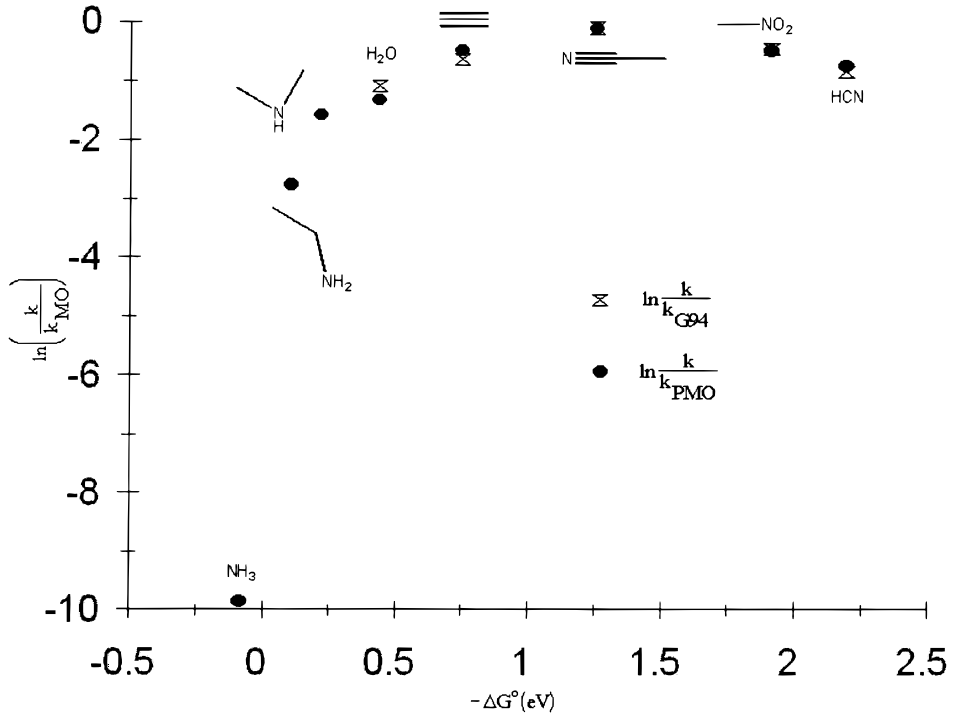

Figure 3. Natural log of reaction efficiency, k_{exp}/k_{col}, for hydride reactions with polar molecules, k_{exp} from ref 20 and k_{col} from Table 2.

TABLE 3: PMO and ADO Reaction Efficiency (k_{exp}/k_{coll}) for the Reactions $H^- + HY \rightarrow H_2 + Y^-$ at 297 K[a]

		k_{exp}/k_{coll}			
reactant	k_{exp}[20]	PMO	G94	ADO[8e]	$\Delta G°$ (eV)
HCN	15	0.47	0.43	1.38	2.19
CH_3NO_2	13	0.61	0.63	1.00	1.91
CH_3CN	13	0.89	0.90	0.92	1.26
C_2H_2	4.4	0.62	0.53	0.99	0.747
H_2O	3.7	0.27	0.34	0.52	0.436
$(CH_3)_2NH$	4.3	0.21		0.15	0.218
$C_2H_5NH_2$	1.1	0.063		0.16	0.104
NH_3	9.2×10^{-4}	5.26×10^{-5}		1.4×10^{-4}	−0.083

[a] k_{exp}, the experimental reaction rate constant (10^9 $mol^{-1}\cdot cm^3\cdot s^{-1}$); k_{MO}, k_{PMO}, the calculated (PMO or Gaussian-94) collision rate constants (10^9 $molecule^{-1}\cdot cm^3\cdot s^{-1}$).

between endothermic proton-transfer reactions (very low efficiency) and exothermic proton-transfer reactions, efficiencies near 1.[24]

If the calculated rates in Table 2 are compared with the experimental values, the ADO calculated rates at first seem much closer to the observed rates than those computed by the models presented here. The calculated rates are only the collision rates. The reaction rates are the collision rates multiplied by the reaction efficiency. In the development of the ADO model the implicit assumption was that the reaction efficiency was approximately unity for all exothermic reactions.[2] This assumption guided the parametrization of the method and resulted in reaction efficiencies greater than 1 for the most exothermic reactions (see Table 3). The implicit assumption that gas-phase reaction efficiencies should be approximately 1 for all exothermic reactions is the equivalent of saying that all such reactions have the same density of states.[23] The density of states must vary dramatically for reactions whose exothermicities differ by the order of an electronvolt. Their reaction efficiencies cannot be the same.

If the reaction efficiency is restricted to be not greater than 1 for the ADO calculation, the natural logs of the reaction efficiency for the PMO and ADO calculations are similar. However, the latter set of calculations increase monotonically with increasing exothermicity. It would be surprising if the calculations did not produce similar results, because both have been adjusted to simulate the observed reality. The maximum value in the PMO calculation is obtained for acetonitrile, −0.117, exothermicity 1.26 eV. The corresponding maximum, 0, is obtained for HCN in the ADO calculation, exothermicity 2.19 eV. If a more exothermic reaction were added to the list, it is likely that the maximum efficiency would shift to that

compound. The result of the most exothermic reaction having the highest reaction efficiency is not realistic in the context of modern theory.

This article presents both PMO and ab initio models for ion-polar-molecule collisions. The PMO model is primarily a heuristic. It is also a simple procedure that can be applied to cases in which ab initio methods fail to converge. The PMO model shows that the collision rate in ion−molecule collisions is controlled by concentrations, masses, charges, dipole moments, moments of inertia, and the energy gap between the frontier orbitals of the ion−molecule complex. It is the last item that is missing from a classical treatment. The ab initio molecular orbital model produces results that are in agreement with the PMO model.

The results in Tables 2 and 3 and Figure 3 show that calculations using an approximate molecular orbital approach, the PMO model, give results for gas-phase reaction efficiencies that compare favorably with results from calculations using Gaussian-94.[22] Both calculations provide reaction efficiencies that are directly in accord with modern kinetic theories.[23] Golden Rule kinetic theories require that gas-phase reactions show a maximum in rate constant (reaction efficiency) as a function of free energy.[23] Previous treatments of ion-polar molecule collision rates either assumed unit reaction efficiencies for all exothermic reactions, or produce reaction efficiencies that increase with increasing $-\Delta G°$ for the reaction. PMO and ab initio calculations of ion polar molecule collision rates using a classical Stark effect model for the ion−dipole interaction give reaction efficiencies that maximize at $-\Delta G° \sim 1.3$ eV. Both the position of the maximum and shape of the curve are congruent with expectations based on Golden Rule theories of chemical rate processes.[23]

Conclusions

A perturbation molecular orbital model has been developed for ion polar molecule capture collisions. The model replaces the induced dipole potential in the Langevin treatment with a perturbation molecular orbital potential. The effect of the ion−dipole interaction on the collision rate is modeled using the formalism of the Stark effect. The model conserves both energy and angular momentum. The results from the PMO model are in good agreement with those obtained using an ab initio model. Reaction efficiencies derived by this model are congruent with expectations of modern chemical reaction rate theories.

References and Notes

(1) Langevin, M. P. *Ann. Chim. Phys*. **1905**, *5*, 245.

(2) Su, T.; Bowers, M. T. Classical Ion−Molecule Collision Theory. In *Gas-Phase Ion Chemistry*; Bowers, M. T., Ed.; Academic Press: New York; 1979; Vol. 1, p 83.

(3) Ridge, D. P. Capture Collision Theory. In *Structure/Reactivity and Thermo-Chemistry of Ion*; Ausloos, P., Lias, S. G., Eds.; *Proceedings of a NATO Advanced Study Institute*, Les Arcs, France, 1987.

(4) (a) Su, T.; Bowers, M. T. *J. Chem. Phys*. **1973**, *58*, 3027; (b) Bass, l.; Su, T.; Chesnavich, W. J.; Bowers, M. T. *Chem.* Phys. Lett. **1975**, *34*, 119; (c) Su, T.; Bowers, M. T. *Int. J. Mass Spectrom. Ions Phys.*, **1973**, *12*, 347.

(5) Su, T.; Bowers, M. T. *J. Chem. Phys.* **1978**, *69*, 2243.

(6) Barker, R. A.; Ridge, D. P. *J. Chem. Phys.* **1976**, *64*, 4411.

(7) (a) Truuski, J.; Forys, M. *J. Phys. Chem.* **1979**, *83*, 2815; (b) Cell, F.; Weddle, G.; Ridge, D. P. *J. Chem. Phys.* **1980**, *73*, 801.

(8) (a) Dugan, J. V.; Magee, J. L. *J. Chem. Phys.* **1967**, *47*, 3103; (b) Linde, R. S. V.; Hase, W. L. *J. Chem. Phys.* **1990**, *93*, 7962; (c) Chesnavich, W. J.; Bowers, M. T. *J. Chem. Phys.* **1978**, *66*, 901; (d) Chesnavich, W. J.; Su, T.; Bowers, M. T. *J. Chem. Phys*. **1980**, *72*, 2641; (e) Su, T.; Chesnavich, W. J. *J. Chem. Phys*. **1982**, *76*, 5183; (f) Su, T. *J. Chem. Phys.* **1994**, *100*, 4703.

(9) (a) Bates, D. R. *Chem. Phys. Lett.* **1981**, *82*, 396; (b) Bates, D. R.; Morgan, W. L. *J. Chem. Phys.* **1987**, *87*, 2611.

(10) (a) Sakimoto, K.; Takaynagi, K. *Chem. Phys.* **1984**, *85*, 273; (b) Sakimoto, K. *Chem. Phys. Lett*. **1985**, *116*, 96.

(11) (a) Troe, J. *Chem. Phys. Lett*. **1985**, *122*, 425; (b) Troe. J. *J. Chem. Phys*. **1996**, *108*, 6429.

(12) Wollrab, J. E. *Rotational Spectra and Molecule Structure*; Academic Press: New York, 1967.

(13) Dougherty, R. C.; Xu, M. *J. Am. Chem. Soc*. **1996**, *118*, 9424.

(14) Dewar, M. J. S.; Dougherty, R. C. *The PMO Theory of Organic Chemistry*; Plenum: New York, 1975.

(15) Coulson, C. A. *Valence, 2nd ed.*; Oxford University Press: New York, 1965.

(16) Gioumousis, G.; Stevenson, D. P. *J. Chem. Phys*. **1958**, *29*, 294.

(17) McLafferty, F. W.; Michnowicz, J. A. *Chem. Technol*. **1992**, *22*, 182.

(18) Lias, S. G.; Bartmess, J. E.; Liebman, J. F.; Levin.R. D.; Mallard W. G. *J. Phys. Chem. Ref. Data* **1988**, suppl. 1.

(19) Moore , W. J. *Physical Chemistry*, 4th ed.; Prentice-Hall: New York, 1962.

(20) Bohme, D. K. *Ion−Molecule Reaction Rate Measurements at York University* through 1981; Ion Chemistry Laboratory, York University: Ontario, Canada, 1982.

(21) Belson, R. D.; Lide, D. R.; Maryott, A. A. *Natl. Stand. Ref. Data Ser*. **1967**, 10.

(22) Frisch, M. J.; Trucks, G. W.; Schlegel, H. B.; Gill, P. M. W.; Johnson, B. G.; Robb, M. A.; Cheeseman, J. R.; Keith, T.; Petersson, G. A.; Montgomery, J. A.; Raghavachari, K.; Al-Laham, M. A.; Zakrewski, V. G.; Ortiz, J. V.; Foresman, J. B.; Cioslowski, J.; Stefanov, B. B.; Nanayakkara, A.; Challacombe, M.; Peng, C. Y.; Ayala, P. Y.; Chen, W.; Wong, M. W.; Andres, J. L.; Reploge, E. S.; Gomperts, R.; Martin, R. L.; Martin, D. L.; Fox, D. J.; Binkley, J. S.; Defrees, D. J.; Baker, J.; Stewart, J. P.; Head-Gordon, M.; Gonzalez, C.; and Pople, J. A. *Gaussian 94*; Gaussian, Inc.: Pittsburgh, PA, 1995.

(23) (a) Marcus, R. A. *Angew. Chem., Int. Ed. Engl.* **1993**, *32*, 1111; (b) Devault, D. *Quantum-Mechanical Tunneling in Biological Systems*, 2nd ed.; Cambridge University Press: Cambridge, 1984.

(24) (a) Bohme, D. K.; Mackay, G. I.; Schiff, H. I. *J. Chem. Phys*. **1980**, *73*, 4976−4982; (b) Bohme, D. K. *Trans R. Soc. Can. Sect. 4* **1981**, *XIX*, 265−272.